

**Figure 2.** Effect of solvent hydrophobicity on the catalytic activity of peroxidase with *p*-cresol as substrate. The units of  $V_{\max}$  are  $\mu\text{mol}(\text{mg enzyme})^{-1}\text{ s}^{-1}$ .

nitude) in organic solvents as compared to aqueous buffer. Furthermore, in all solvents, catalytic efficiency decreased as substrate hydrophobicity increased. This substrate effect, however, became more pronounced as solvent hydrophobicity increased; the slopes of catalytic efficiency vs  $\pi$  became more negative as a function of  $\log P$  (Figure 1C), and with high linearity (correlation coefficient of 0.98), neglecting the dioxane-water mixtures.<sup>11</sup> These results indicate that a linear free energy relationship exists between catalytic efficiency and *both* substrate and solvent hydrophobicities. Furthermore, substrate hydrophobicity becomes a significant reaction variable as solvent hydrophobicity increases. The above findings may be explained purely by the partitioning behavior of phenols between the bulk reaction medium and the peroxidase active site. This partitioning is likely to diminish as substrate and solvent hydrophobicities increase, thereby necessitating a larger concentration of phenols to saturate the enzyme. This results in an increase in the apparent  $K_m$  of the phenols in organic versus aqueous media.<sup>13</sup>

The  $K_m$  effect was verified by calculation of the values of apparent  $K_m$ . All phenols tested have significantly higher apparent  $K_m$ 's in organic solvents than in water. In some cases, this increase is over 3 orders of magnitude. For example, in aqueous buffer, the apparent  $K_m$ 's of *p*-methoxyphenol, *p*-cresol, *p*-ethylphenol, and *p*-propylphenol are 0.63, 0.70, 0.25, and 0.15 mM, respectively. In butyl acetate, however, the apparent  $K_m$ 's were 28, 42, 110, and 250 mM for the same phenols, respectively. Furthermore, these differences become more pronounced as the phenolic substituent becomes more hydrophobic, as would be expected if substrate partitioning into the peroxidase's active site were disrupted by solvent hydrophobicity.

Taking advantage of the high solubilities of phenols in organic solvents, we investigated the solvent effect on catalytic activity,  $V_{\max}$ . Inspection of the data for *p*-cresol oxidation in aqueous and organic media (Figure 2) reveals that catalytic activity is *stimulated* in several organic solvents. Hence, peroxidase retains its full catalytic power in a variety of nonaqueous solvents. Peroxidase

(11) We speculate that the dioxane anomaly is due to a conformational change in the enzyme. While enzymes in water-immiscible solvents appear to retain their native structural integrity<sup>1,2b,c,12</sup> and are rigid, the high water content used in the dioxane solvent systems (5–30%, v/v) may have allowed the peroxidase to become more mobile than in a less hydrated, water-immiscible solvent and thereby adopt an altered conformation.

(12) Zaks, A.; Klibanov, A. M. *Proc. Natl. Acad. Sci. U.S.A.* **1985**, *82*, 3192–3196. Zaks, A.; Klibanov, A. M. *J. Biol. Chem.* **1988**, *263*, 3194–3201. Clark, D. S.; Creagh, L.; Skerker, P.; Guinn, M.; Prausnitz, J.; Blanch, H. In *Biocatalysis and Biomimetics*; Burrington, J. D., Clark, D. S., Eds.; ACS Symposium Series 392; American Chemical Society: Washington, DC, 1989. Kanerva, L. T.; Klibanov, A. M. *J. Am. Chem. Soc.* **1989**, *111*, 6864–6865.

(13) Similar increases in apparent  $K_m$  have been observed for trypsin catalysis in dioxane-water mixtures (Douzou, P.; Balny, C. *Proc. Natl. Acad. Sci. U.S.A.* **1977**, *74*, 2297–2300).

(14) This work was financially supported by the National Science Foundation (Grant CBT-8808897), the Mead Corporation, and the donors of the Petroleum Research Fund, administered by the American Chemical Society.

does require added water for activity, however. No reaction is observed in water-miscible solvents in the absence of added water, and catalysis in water-immiscible solvents requires a small amount of water.<sup>7</sup>

Our findings demonstrate that peroxidase catalysis in organic solvents can occur with full inherent catalytic turnover. The major effect of the solvent is to cause a dramatic increase in apparent  $K_m$  values. Furthermore, peroxidase catalysis in organic media follows a linear free energy relationship between catalytic efficiency and substrate and solvent hydrophobicities. This finding, if general (currently under investigation with other enzymes), can be used to develop rational mathematical descriptions of enzymatic catalysis in nonaqueous media in order to optimize enzyme function.

### A Novel Coordination Mode for Oxygen: Preparation and Properties of $(\text{NBu}^n_4)_2[\text{V}_4\text{O}(\text{edt})_2\text{Cl}_8]$ Containing a Square-Planar Oxide Bridge

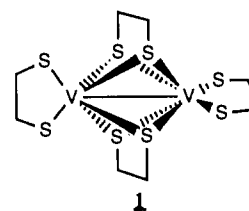
Joe R. Rambo,<sup>1a</sup> John C. Huffman,<sup>1b</sup> and George Christou<sup>\*,1a,d</sup>

Department of Chemistry and the Molecular Structure Center, Indiana University  
Bloomington, Indiana 47405

Odile Eisenstein<sup>1c</sup>

Laboratoire de Chimie Theorique  
Centre de Paris-Sud, 91405 Orsay, France  
Received May 4, 1989

We are currently engaged in a program directed toward the development of V/S chemistry. In earlier reports we described several V/S complexes encompassing nuclearities 1–4 and oxidation levels III–V, including mixed valency.<sup>2–8</sup> Among these is the dinuclear V<sup>III</sup> complex  $(\text{PPh}_4)_2[\text{V}_2(\text{edt})_4]$  (1; edt = eth-



ane-1,2-dithiolate)<sup>6,8–10</sup> whose diamagnetism and V...V separation (ca. 2.6 Å) suggest a rare example of V<sup>III</sup> metal-metal bonding. This complex also possesses an unusual metal coordination geometry and a quadruply bridged core. The latter properties are probably the cause of the V...V separation being longer than expected for a d<sup>2</sup>-d<sup>2</sup> double bond (ca. 2.4 Å).<sup>11</sup> In subsequent

(1) (a) Indiana University, Chemistry Department. (b) Indiana University, Molecular Structure Center. (c) Centre de Paris-Sud. (d) Alfred P. Sloan Fellow, 1987–1989; Camille and Henry Dreyfus Teacher-Scholar, 1987–1992.

(2) Money, J. C.; Huffman, J. C.; Christou, G. *Inorg. Chem.* **1985**, *24*, 3297.

(3) Money, J. K.; Nicholson, J. R.; Huffman, J. C.; Christou, G. *Inorg. Chem.* **1986**, *25*, 4072.

(4) Money, J. K.; Huffman, J. C.; Christou, G. *J. Am. Chem. Soc.* **1987**, *109*, 2210.

(5) Money, J. K.; Folting, K.; Huffman, J. C.; Christou, G. *Inorg. Chem.* **1987**, *26*, 944.

(6) Money, J. K.; Huffman, J. C.; Christou, G. *Inorg. Chem.* **1988**, *27*, 507.

(7) Nicholson, J. R.; Huffman, J. C.; Ho, D.; Christou, G. *Inorg. Chem.* **1987**, *26*, 3030.

(8) Wiggins, R. W.; Huffman, J. C.; Christou, G. *J. Chem. Soc., Chem. Commun.* **1983**, 1313.

(9) (a) Pulla Rao, Ch.; Dorfman, J. R.; Holm, R. H. *Inorg. Chem.* **1986**, *25*, 428. (b) Dorfman, J. R.; Holm, R. H. *Inorg. Chem.* **1983**, *22*, 3179.

(10) Szymies, D.; Krebs, B.; Henkel, G. *Angew. Chem., Int. Ed. Engl.* **1983**, *22*, 885.

(11) Indeed EHT calculations suggest the metal-metal interaction is better described as a single bond. See ref 9b.

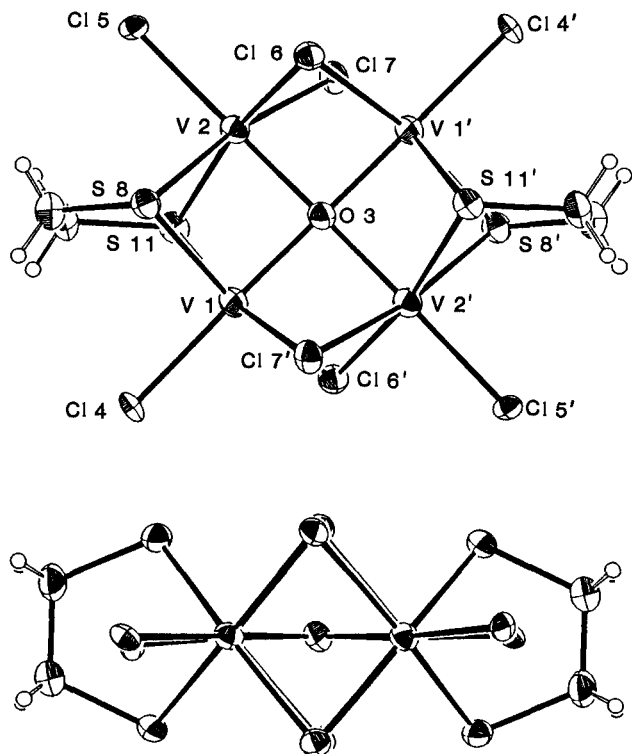


**Figure 1.** ORTEP representations of the anion of complex **2** showing both top and side views to emphasize the planarity of the  $V_4O$  unit. Selected distances (Å) and angles (deg): V1–V2, 2.8637 (13); V1–V2', 2.8090 (15); V1–O3, 2.0135 (10); V2–O3, 1.9978 (9); V1–Cl(4,6,7), 2.3448 (15), 2.4227 (19), 2.4381 (11); V1–S(8,11), 2.4092 (19), 2.4164 (12); V2–Cl(5,6,7), 2.3303 (15), 2.4551 (16), 2.4487 (16); V2–S(8,11), 2.4254 (17), 2.4257 (17); V1–O3–V2, 91.11 (4); V1–O3–V2', 88.89 (4); V1–S8–V2, 72.64 (4); V1–S11–V2, 72.52 (5); V1–Cl6–V2', 70.32 (4); V1–Cl7–V2', 70.17 (5); V1–V2–V1', 90.45 (4); V2–V1–V2', 89.55 (4).

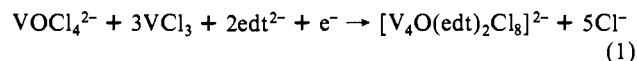
studies, we investigated whether lowering of the  $edt^{2-}:V$  ratio would yield a mixed  $Cl^-/edt^{2-}$  dinuclear complex with a different structural core to **1** and wondered how this might affect the  $V\dots V$  separation. We herein report that the product from one such reaction is not dinuclear but tetranuclear,  $(NBu^i)_2[V_4O(edt)_2Cl_8]$  (**2**), containing the first example of a square-planar oxide in a molecular species.

After some preliminary investigation of different reagent ratios and solvent, reaction of  $VCl_3$ ,  $Na_2edt$ , and  $NBu^i_4Cl$  in a 2:1:1 ratio in  $CH_2Cl_2$  for 48 h followed by filtration and careful layering of the dark brown filtrate with  $Et_2O$  yielded black crystals of **2** in ~30% yield. IR data and elemental analysis<sup>12</sup> indicated **2** not to be a known  $V/edt^{2-}$  complex, and its precise identity was therefore investigated by crystallography.<sup>13</sup> The structure of the anion is shown in Figure 1. The tetranuclear unit lies on an inversion center yielding an exactly planar, approximately square  $V_4^{III}$  unit. The four edges are bridged by four  $Cl^-$  and two  $edt^{2-}$  groups, the latter in the same  $\eta^2, \eta^2, \mu_2$ -mode as in **1**. Each V possesses one terminal  $Cl^-$  ligand, and lying on the inversion center is a  $\mu_4-O^{2-}$  completing approximately octahedral metal geometry. The anion has virtual  $D_{2h}$  symmetry. The source of the  $\mu_4-O^{2-}$  is most probably adventitious  $H_2O$ ; as we have found previously when adventitious O was detected in a product,<sup>5</sup> we have been unable to obtain an oxide-free product under more anoxic/anhydrous conditions.<sup>14</sup>

(12) Calculated for  $C_{36}H_{80}N_2OCl_8S_4V_4$ : C, 36.87; H, 6.88; N, 2.39; Cl, 24.18; V, 17.38. Found: C, 36.97; H, 6.80; N, 2.51; Cl, 24.8; V, 17.2.

(13) Crystal data:  $C_{36}H_{80}N_2O_8S_4Cl_8V_4$ , triclinic,  $P\bar{1}$ ,  $T = -155^\circ C$ ,  $a = 12.584(2)$  Å,  $b = 11.421(2)$  Å,  $c = 11.204(2)$  Å,  $\alpha = 67.12(1)^\circ$ ,  $\beta = 110.59(1)^\circ$ ,  $\gamma = 110.60(1)^\circ$ ,  $V = 1345.02$  Å<sup>3</sup>,  $Z = 1$ ,  $6^\circ \leq 2\theta \leq 45^\circ$ , unique data = 3500, obsd data = 3087,  $F > 2.33\sigma(F)$ . The structure was solved by direct methods (MULTAN) and Fourier techniques and refined by full-matrix least squares. All non-hydrogen atoms were refined anisotropically; all hydrogen atoms were located and refined isotropically in the final cycles. Final  $R(R_w) = 4.26(4.78)\%$ .

With the identity of **2** established, it was now felt important to develop a rational procedure for its synthesis. We have previously shown that  $V_2O(aet)_4$  ( $aet^- = 2$ -aminoethanethiolate) and  $V_2(edt)_4^{2-}$  can be prepared by reduction of the vanadyl complexes  $VO(aet)_2$  and  $VO(edt)_2^{2-}$ , respectively.<sup>5</sup> A similar reaction has provided the desired rational synthesis of complex **2**. A mixture of  $(NBu^i)_2[VOCl_4]$ ,  $VCl_3(thf)_3$ , and  $Na_2(edt)$  (1:3:2) in  $CH_3CN$  was treated with 1 equiv of  $NaACN$  (0.5 M solution in THF;  $ACN^- =$  acenaphthylenide). The brown solution was filtered and, after unexceptional workup, gave complex **2** in 70–75% yield. This procedure (eq 1) involves reductive activation or destabilization<sup>15</sup>



of the multiply bonded  $VO^{2+}$  unit, triggering aggregation and conversion of the terminal  $O^{2-}$  into a  $\mu_4$ -bridging mode.

Complex **2** is the first example of a square-planar oxide in a molecular species. The known examples are the nonmolecular solids  $MO$  ( $M = Nb, Ti$ )<sup>16a-f</sup> and  $Sc_{0.75}Zn_{1.25}Mo_4O_7$ .<sup>16g</sup> In  $NbO$ , all Nb and O centers are square planar, and this remarkable structure has been shown to be stabilized by enhanced Nb–Nb bonding and Nb–O  $\pi$ -bonding.<sup>17</sup> To similarly assess the importance of such factors in stabilizing **2** and to characterize, in general, the electronic nature of this unusual bridging mode for oxygen, we have carried out EHT calculations on the model complex  $[V_4O(SH)_4Cl_8]^{2-}$  with idealized  $D_{2h}$  symmetry. The fragment without the  $O^{2-}$  atom was also calculated to analyze the interactions between the  $V_4$  cage and its occupant  $O^{2-}$ . The V–V bond order is hardly affected by the  $O^{2-}$ ; the former is relatively small so that no strong V–V bonding is present. The stability of the complex is undoubtedly due to the large V–O bonding interaction as evidenced by the Mulliken Overlap Population and the availability of low-lying empty orbitals of proper symmetry to efficiently stabilize the s,  $p_x$ ,  $p_y$ , and  $p_z$  orbitals of the oxygen in its unusual square-planar geometry. The metal-centered orbitals of the O-free cage are the symmetry-adapted linear combinations of the four metal orbitals.<sup>18</sup> This gives an energetically closely spaced band of 16 orbitals, four of which are occupied.<sup>19</sup> The orbitals adapted to strongly interact with the oxygen atom are easily assigned. The four metal  $\sigma$  hybrids play a major role, for they combine to give an  $a_{1g}$ ,  $e_u$ , and  $b_{1g}$  set (Figure 2). The  $a_{1g}$  and  $e_u$  orbitals are ideally suited to strongly stabilize the O s,  $p_x$ , and  $p_y$  orbitals, respectively. The O  $p_z$  orbital is stabilized by an empty  $a_{2u}$  orbital. This  $\pi$  interaction is smaller than those involving the O s,  $p_x$ , and  $p_y$  orbitals which are of  $\sigma$  character and comprise the majority of the O-to- $V_4$  electron donation. The total O-to- $V_4$  electron donation is significant and represents clear evidence for the importance of the O to the stability of the cluster.

The majority of the closely spaced metal orbitals do not possess the proper symmetry for interacting with the O and remain at the frontier level. This leads to an insignificant HOMO–LUMO gap and rationalizes the observed paramagnetism of complex **2**<sup>20</sup>

(14) One reaction was even carried out in the presence of  $Li_2S$ ; complex **2** was nevertheless the identity of the isolated material.

(15) Taking the  $VO^{2+}$  vector as the z axis and the basal ligands to lie on the x, y axes, the unpaired electron will reside in the  $d_{xy}$  orbital. Since V is a 3d metal, the  $d_{xy} \rightarrow d_{xz}, d_{yz}$  separation would not be expected to be large enough to cause spin-pairing. As a result, the added electron will enter the  $d_{xz}, d_{yz}$  orbitals (degenerate under  $C_{4v}$  symmetry) which are strongly  $\pi^*$  with respect to V–O bonding. This will destabilize the  $VO^{2+}$  multiply bonded unit and trigger conversion of O into a bridging mode. No examples of terminal  $VO^{2+}$ -containing complexes are known.

(16) (a) Wells, A. F. *Structural Inorganic Chemistry*, 5th ed.; Clarendon: Oxford, 1984. (b) Brauer, G. *Z. Anorg. Allg. Chem.* **1941**, *248*, 1. (c) Anderson, G.; Magneli, A. *Acta Chem. Scand.* **1957**, *11*, 1065. (d) Watanabe, D.; Terasaki, O.; Jotsons, A.; Castles, J. R. *J. Phys. Soc. Jpn.* **1968**, *25*, 292. (e) Watanabe, D.; Castles, J. R.; Jotsons, A.; Malin, A. S. *Acta Crystallogr.* **1967**, *23*, 307. (f) Hilti, E. *Naturwissenschaften* **1968**, *55*, 130. (g) McCarty, R. E. *Polyhedron* **1986**, *5*, 51.

(17) Burdett, J. K.; Hughbanks, T. *J. Am. Chem. Soc.* **1984**, *106*, 3101.

(18) The three low-lying nonbonding orbitals ( $t_{2g}$ ) of the square pyramid and the  $\sigma$  hybrid pointing toward the center of the cage.

(19) Due to the closeness in energy of this band of orbitals, it is beyond the accuracy of the EHT method to ascertain with safety which ones are occupied and which are empty in this fragment.

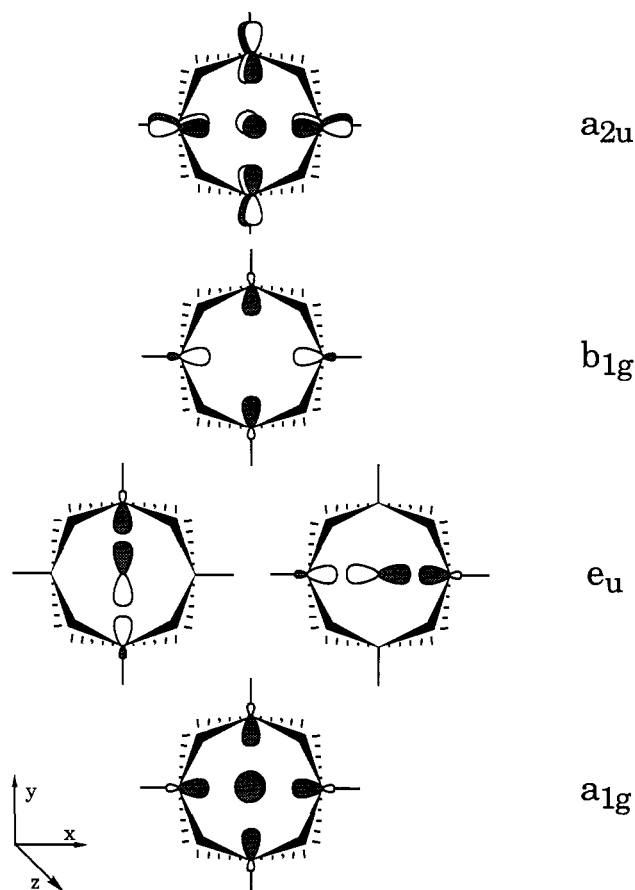


**Figure 2.** Depiction of the five orbitals referred to in the text. This figure and the text discussion employ  $D_{4h}$  notation for convenience in axis labeling and to emphasize that the O  $p_x$  and  $p_y$  orbitals are playing essentially equivalent roles. The calculations were actually performed on the  $D_{2h}$  model complex (see text), but the lowering of symmetry is minimal and the orbitals are almost of  $D_{4h}$  symmetry.

which is assigned to the thermal population of low-lying empty orbitals. There also seems no apparent reason why other ions with appropriate orbitals could not be embedded in the  $V_4$  cage provided that enough space is available.<sup>21</sup>

Finally, what of our original thought that a lower  $edt^{2-}:V$  ratio might yield a metal-metal bonded mixed  $Cl^-/edt^{2-}$  dinuclear species. Inspection of Figure 1 makes it tempting to speculate that such a species may indeed have formed as an intermediate (viz.  $[V_2(\mu-edt)(\mu-Cl)_2Cl_4]^{2-}$  or similar) that then "dimerized" to **2** with incorporation of adventitious O. To evaluate this possibility, the  $V:edt^{2-} = 2:1$  and  $1:1$  reactions are currently under further investigation.

**Acknowledgment.** This work was supported by the Office of Basic Energy Sciences, Division of Chemical Sciences, U.S. Department of Energy under Grant DE-FG02-87ER13702. We thank James D. Martin for assistance with the MO calculations. The Laboratoire de Chimie Theorique is associated with the CNRS (UA 506) and is a member of ICMO and IPCM. We thank NSF and CNRS for support under the U.S.-France Cooperative Science Program.

**Registry No. 2,** 122489-65-0.

**Supplementary Material Available:** Tables of fractional coordinates and isotropic and anisotropic thermal parameters (3 pages). Ordering information is given on any current masthead page.

(20) An Evans method determination in  $CD_3CN$  gave a value of ca.  $2.0 \mu_B/V$ .

(21) Note that an example of a square-planar  $OH^-$  has recently been reported: McKee, V.; Tandon, S. S. *J. Chem. Soc., Chem. Commun.* **1988**, 385.

## UV Endonuclease V from Bacteriophage T<sub>4</sub> Catalyzes DNA Strand Cleavage at Aldehydic Abasic Sites by a Syn $\beta$ -Elimination Reaction

Abhijit Mazumder and John A. Gerlt\*

Department of Chemistry and Biochemistry  
University of Maryland  
College Park, Maryland 20742

Lois Rabow

Department of Biochemistry, University of Wisconsin  
Madison, Wisconsin 53706

Michael J. Absalon and JoAnne Stubbe

Department of Chemistry  
Massachusetts Institute of Technology  
Cambridge, Massachusetts 02139

Philip H. Bolton

Department of Chemistry, Wesleyan University  
Middletown, Connecticut 06457

Received May 2, 1989

We recently reported unequivocal evidence that UV endonuclease V from bacteriophage T<sub>4</sub> (UV endo V) cleaves the phosphodiester bond on the 3'-side of an aldehydic abasic site in a DNA heteroduplex via a novel  $\beta$ -elimination mechanism.<sup>1,2</sup> We now report determination of the stereochemical course of the elimination reaction. Stereospecifically tritiated abasic sites in polymers prepared from samples of poly(dA-dU) were used to probe the stereospecificity of hydrogen abstraction; UV endo V abstracts the *pro-S* 2-hydrogen. <sup>1</sup>H NMR spectroscopy of the product obtained from unlabeled polymer revealed that the  $\alpha,\beta$ -unsaturated aldehyde has the *trans* geometry. Thus, the stereochemistry of the  $\beta$ -elimination reaction is *syn*, and this indicates that the reaction proceeds from an acyclic species derived from the mixture of cyclic hemiacetals which predominates in solution.<sup>3</sup>

The choice of substrate for these studies was based on the availability of samples of dUTP stereospecifically labeled with <sup>3</sup>H in either the *pro-S* or *pro-R* 2'-hydrogen.<sup>4</sup> In the presence of a template, the Klenow fragment of DNA polymerase from *Escherichia coli* synthesizes poly(dA-dU) from dATP and dUTP.<sup>5</sup> Three samples of poly(dA-dU) were prepared: no label in dU, <sup>3</sup>H in the *pro-S* 2'-hydrogen of dU, and <sup>3</sup>H in the *pro-R* 2'-hydrogen of dU. The uracil present in these polymers was quantitatively removed by the action of uracil-DNA glycosylase from *E. coli*.<sup>6</sup> These "damaged" and presumably single-stranded polymers are substrates for UV endo V and can be completely degraded to a single product.

The polymer containing <sup>3</sup>H in the *pro-R* 2-hydrogen of the abasic site (specific radioactivity, 44 000 cpm/ $\mu$ mol) was converted by UV endo V<sup>7</sup> into a tritiated nucleotide ester product (specific

(1) Manoharan, M.; Mazumder, A.; Ransom, S. C.; Gerlt, J. A.; Bolton, P. H. *J. Am. Chem. Soc.* **1988**, *110*, 2690-2691.

(2) Two other laboratories have concluded that UV endo V, the UV endonuclease from *Micrococcus luteus*, and endonuclease III from *Escherichia coli* (Bailey, V.; Verly, W. G. *Biochem. J.* **1987**, *242*, 565-572. Kim, J.; Linn, S. *Nucleic Acids Res.* **1988**, *16*, 1135-1141. Bailey, V.; Sente, B.; Verly, W. G. *Biochem. J.* **1989**, *259*, 751-759) catalyze  $\beta$ -elimination reactions. These conclusions were based upon the chromatographic properties of the sugar-phosphate product as well as the labilization of <sup>3</sup>H from abasic sites labeled in the both the 1-position (40%) and the *pro-R* 2-position (60%). The structure of the sugar-phosphate product was not actually determined. The stereospecificity of <sup>3</sup>H abstraction by UV endo V that was implicitly determined by Bailey et al. is inconsistent with the results we are now reporting.

(3) Wilde, J. A.; Bolton, P. H.; Mazumder, A.; Manoharan, M.; Gerlt, J. A. *J. Am. Chem. Soc.* **1989**, *111*, 1894-1896.

(4) The synthesis of [<sup>2'(R)</sup>-<sup>3</sup>H]dUTP was accomplished by the reduction of UTP in <sup>3</sup>H<sub>2</sub>O catalyzed by ribonucleoside triphosphate reductase from *Lactobacillus leichmannii*. The synthesis of [<sup>2'(S)</sup>-<sup>3</sup>H]dUTP is described in the supplementary material.

(5) Setlow, P.; Brutlag, D.; Kornberg, A. *J. Biol. Chem.* **1972**, *247*, 224-231.

(6) The conditions for the uracil-DNA glycosylase reaction and the analytical methods used to follow the progress of the reaction are available in the supplementary material.